Proceedings of the XVIII ECSMGE 2024
GEOTECHNICAL ENGINEERING CHALLENGES
TO MEET CURRENT AND EMERGING NEEDS OF SOCIETY

ISBN 978-1-032-54816-6
DOI 10.1201/9781003431749-552

Back-analysis of a small-scale (1g) energy pile test using the finite element method

Rétro analyse avec la méthode des éléments finis d'un test de pieux énergétique à petite dimension (1g)

P.J. Bourne-Webb*, T.M. Bodas Freitas
CERIS, Instituto Superior Técnico, ULisboa, Lisbon, Portugal

D. Abrantes
Helica, Tomar, Portugal (formerly Instituto Superior Técnico)

**peter.bourne-webb@tecnico.ulisboa.pt*

ABSTRACT: Previous work by the authors reviewed the reported response of full- and small-scale piles in tests in granular soils where they were subject to cyclic thermal loading. In the case of the former, largely stable behaviour has been reported but amongst the latter, the reported response consistently reveals irrecoverable settlement and increase in axial compression stress. This later is reported to be a function of the applied load with greater irrecoverable settlement occurring at lower global factor of safety and has been attributed to a variety of possible mechanisms. A hypothetical mechanism based on the initial mobilisation of the pile shaft resistance was proposed to explain this and then tested by undertaking numerical analysis. This confirmed the stable behaviour of the full-scale piles was likely due to low mobilisation (high margin of safety) with respect to the shaft resistance, while in the small-scale tests, the reverse was true. In this paper, a small-scale test on a thermally-activated pile has been back-analysed. In the test, the mechanical load-displacement behaviour along with the response to three cycles of heating and cooling were reported in sufficient detail to provide a good basis for the analytical work. It is shown that by matching the mechanical response, reasonable agreement between the thermal part of the test and finite element back-analysis can be achieved, and that the agreement can be further improved through calibration of the coefficient of thermal expansion of the pile and soil.

RÉSUMÉ: Des travaux antérieurs des auteurs ont examiné la réponse rapportée des pieux à grande et petite échelle lors d'essais dans des sols granulaires où ils étaient soumis à une charge thermique cyclique. Dans le cas des premiers, un comportement largement stable a été rapporté, mais parmi les seconds, la réponse rapportée révèle systématiquement un tassement irrécupérable et une augmentation de la contrainte de compression axiale. Ce dernier est signalé comme étant une fonction de la charge appliquée avec un tassement irrécupérable plus important se produisant à un facteur de sécurité global inférieur et a été attribué à une variété de mécanismes possibles. Un mécanisme hypothétique basé sur la mobilisation initiale de la résistance du fût du pieu a été proposé pour expliquer cela, puis testé en entreprenant une analyse numérique. Cela a confirmé que le comportement stable des pieux à grande échelle était probablement dû à une faible mobilisation (marge de sécurité élevée) par rapport à la résistance de l'arbre, alors que dans les essais à petite échelle, l'inverse était vrai. Dans cet article, un essai à petite échelle sur un pieu activé thermiquement a été rétro-analysé. Dans le test, le comportement mécanique de charge-déplacement ainsi que la réponse à trois cycles de chauffage et de refroidissement ont été rapportés de manière assez détaillée, fournissant une bonne base pour le travail analytique. Il est démontré qu'en faisant correspondre la réponse mécanique, un accord raisonnable entre la partie thermique de l'essai et la rétro-analyse par éléments finis peut être obtenu, et que l'accord peut être encore amélioré par l'étalonnage du coefficient de dilatation thermique du pieu et du sol.

Keywords: Piles; thermal; interactions; safety.

1 INTRODUCTION

In the last decade, numerous (more than 50) experimental studies examining the response of thermally-activated (TA) piles either at 1-g or in the centrifuge at N-g acceleration have been published. Such testing is promoted as being able to provide valuable insights into the response of geotechnical structures in a more controlled and cost-effective manner than e.g. full-scale tests in the field.

Bourne-Webb et al. (2019) and Bourne-Webb & Bodas Freitas (2020) collated the results for such studies, along with full scale tests on TA piles and found a distinct discrepancy between the reported behaviours, especially with respect to the normalised maximum axial thermal stress response ($\sigma_{th,max}/\sigma_{th,fixed}$

where $\sigma_{th,fixed} = \alpha\Delta T.E$; and α = Pile CTE; ΔT = Temp. change; E = pile stiffness; L = pile length) and the likelihood of the pile head movement ($y_{th,0}$) exceeding the free thermal expansion of the pile ($y_{th,free} = \alpha\Delta T.L$), i.e. $y_{th,0}/y_{th,free} > 1$, Figure 1. Reduced axial thermal stress was attributed to the low confining stress acting in 1-g and the very small thermal displacements generated on the model pile interfaces irrespective of scale, due to the short length of the piles. Pile head movement exceeding $y_{th,free}$ was attributed to effects that led to irrecoverable settlement: namely, reduction of available shaft restraint during cooling and load transfer to the pile base, Figure 2.

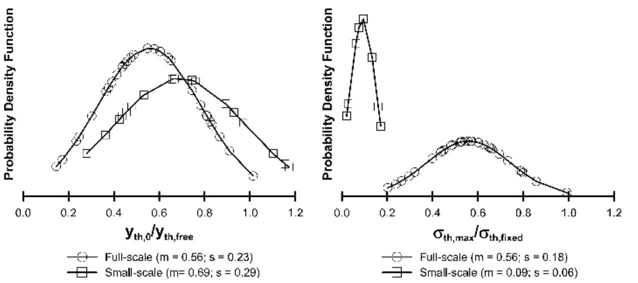

Figure 1. Stress-displacement response of full- and small-scale TA pile tests.

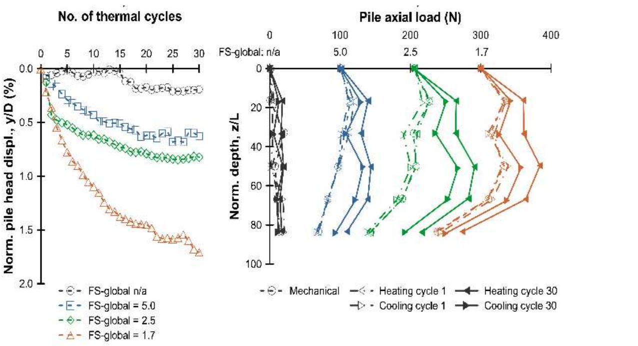

Figure 2. Settlement & axial load response in small-scale cyclically TA pile, Nguyen et al. (2017).

2 BASIS FOR ANALYSES

The model tests used as the basis for this study were those reported by Wang et al. (2016, 2017) in which a single, 104 mm diam., 1.4 m long pile embedded in dry sand was loaded mechanically and then subject to heating and cooling cycles. Specifically, the behaviour of Pile 4 which had a W-shaped heat exchanger tube layout is examined here. In this study, the finite element analysis (FEA) program PLAXIS 2D 2023.1 was employed to undertake the back-analysis of the model test.

The geometry used is based on the physical dimensions of the rectangular test tank which was 1.75 m deep and had plan dimensions of 8 x 8 m^2. While it is possible that the proximity of the lower boundary may have influenced the test results, for this exercise it is not so important as the FEA is replicating the test boundary conditions. The test piles were installed 1 m from the side boundaries and the FEA simplified the geometry to be axisymmetric with a domain radius of 1,0 m (c. 10 pile diameters), Figure 3.

Basic characteristics of the sand used in the testing were reported, along with details of the preparation method and the target initial state: a relative density of about 63%. These details were used to infer suitable parameters to be employed in the back-analysis, Table 1. The stress-dilatancy approach developed by Bolton (1986a, b) was employed to assess the peak angle of shearing resistance that might be applicable in the sand at the very low confining stress in the tank. This suggested a peak angle of shearing resistance of about 40° and thus, a value of φ' = 34° was used in conjunction with an angle of dilation, ψ of 6°, in the FEA. Iwasaki & Tatsuoka (1977) and Mayne (2000) were used to provide an initial estimate for the stiffness parameters, reflecting the confining pressures and level of mobilisation within the model. In the FEA, the Mohr-Coulomb (MC) model available in PLAXIS was employed. These values were then calibrated in order to better reproduce the reported load-displacement of the test piles – primarily through adjusting the soil stiffness and initial stress state.

The thermal and mechanical properties for the model pile were less clearly defined and quoted values in Wang et al. (2016, 2017) appear to be generic rather than model specific, e.g. the quoted coefficient of thermal expansion (CTE) is $10\text{x}10^{-6}\,K^{-1}$ with no mention of their having tested the pile to obtain the value. Likewise, the applicable pile Young's modulus.

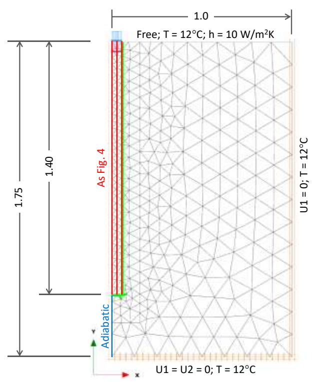

Figure 3. Geometry used in FEA.

Standard mechanical boundary conditions were applied, i.e. fully-fixed on bottom, horizontal fixity on sides and free on the top surface. Regarding temperature boundary conditions, the bottom and outer edge were held constant at 12°C; below the pile, the centreline was set as adiabatic; the surface was set to be convective with a thermal conductance of

10 W/m^2.K and an air-temperature of 12°C. Within the pile, temperatures following the average pile temperaure reported by Wang (2016, 2017) were imposed along lines at x = 0, r/2 and r, where r is the pile radius, Figure 4. This ensured that the pile volume underwent a constant temperature change.

The back-analysis of the model tests was undertaken in two stages: first, the mechanical load-displacement response was evaluated with initial stress, soil shear strength & stiffness parameters calibrated to approximate the response reported by Wang (2016, 2017), then the thermo-mechanical response was evaluated (assuming the above parameters were not affected) with variations in the thermal properties detailed in Section 3. In reproducing the mechanical load-displacement response, the set of parameters finally arrived at included an At-rest Earth Pressure coefficient, K_0 = 1 this is higher than e.g. that given by the Jaky-formula (K_0 = 1-sinφ', Jaky (1948)) but data from Boulon & Foray (1986) show that at low vertical stress, in small scale tests on piles, it is possible to have K_0 values inexcess of 1.0, depending on the density of the soil. So the value used as considered reasonable.

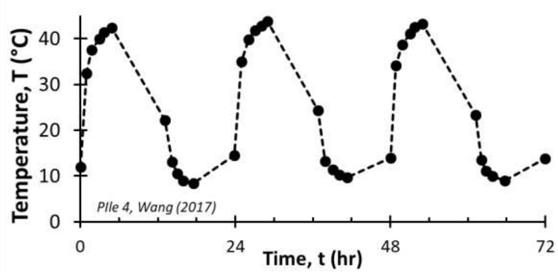

Figure 4. Average pile temperature imposed in FEA, adapted from Wang (2017).

3 RESULTS & DISCUSSION

3.1 Load-displacement response

In Wang et al. (2016, 2017), one model pile was tested in order to define the mechanical behaviour of the pile under axial load. The results were consistent and used to define a working load of 10 kN which was applied to the other test piles before the thermal part of the test was carried out.

After only small alterations in the initiallly assessed soil parameters, acceptable agreement between the reported behaviour and the FEA using both the MC and HS soil models was obtained, Figure 5. This mainly involved, adjustments in the distribution between φ‘ and ψ, and the soil stiffness. From this analysis, it was possible to examine the underlying response which revealed that the available shaft resistance was only a small proportion of the total, around 1,5 to 2 kN, with the remainder derived from the pile base. Thus, a working load of 10 kN, as used by Wang et al. (2016, 2017), implies that the shaft resistance is fully mobilised prior to thermal loading.

3.2 Thermo-mechanical behaviour

Before examining the thermo-mechanical (TM) response, the predicted temperature variation was validated against the radial temperature field reported in Wang (2017). Figure 6 shows this comparison which is very good, confirming that the model is providing an acceptable reproduction of the thermal response. Figure 7 shows the temperature contours for a steady state thermal analysis, to illustrate the effect of the boundary conditions on the temperature field. These fields were the same irrespective of the soil model employed.

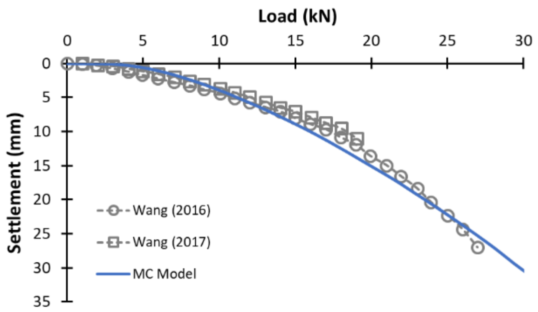

Figure 5. Load-displacement response of model pile as reported in Wang (2016. 2017) and predicted by FEA.

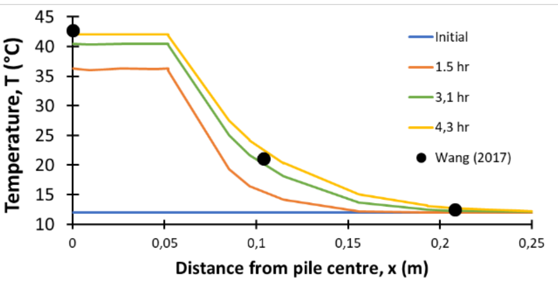

Figure 6. Radial temperature profile at about pile mid-depth, and at the end of first heating stage, reported by Wang (2017) and predicted by FEA.

Having established that the imposed temperature field was acceptable, the thermo-mechanical response was examined via the comparison with reported thermally-induced axial strain (ε_{th}) and stress changes (σ_{th}), and pile head displacement ($y_{0,th}$), and Figure 8 to 10 illustrate the various responses.

Initially, the MC model was employed in conjunction with the CTE of the pile equal to the soil, i.e. 10 x10^{-6} K^{-1}or case "CTE 10/10". First, the axial strain response at a depth of about 0.65 m (0.46L) is compared in Figure 8 and it is apparent that when the pile CTE is 10 x10^{-6} K^{-1} (cases CTE 10/10 & 10/05), the agreement is very good, irrespective of the soil CTE but using a CTE for the pile of 15 x10^{-6} K^{-1} (case CTE 15/10) overestimates the thermal axial strain. This confirms that the value quoted by Wang et al. (2016, 2017) is reasonable. Also shown is the blocked strain, ε_{blkd} (Eq. 1) obtained in the FEA which are rather small and only a few-percent of $\alpha\Delta T$, confirming a lack of restraint on the shaft;

$$\varepsilon_{blkd} = [\varepsilon_{th} - \alpha(T - T_0)] \tag{1}$$

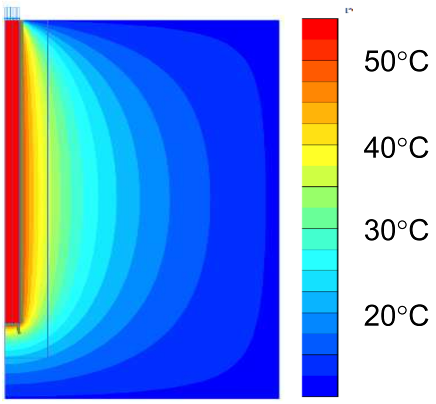

Figure 7. Steady State temperature field for imposed pile temperature of 53 ℃ (ΔT = 41 ℃).

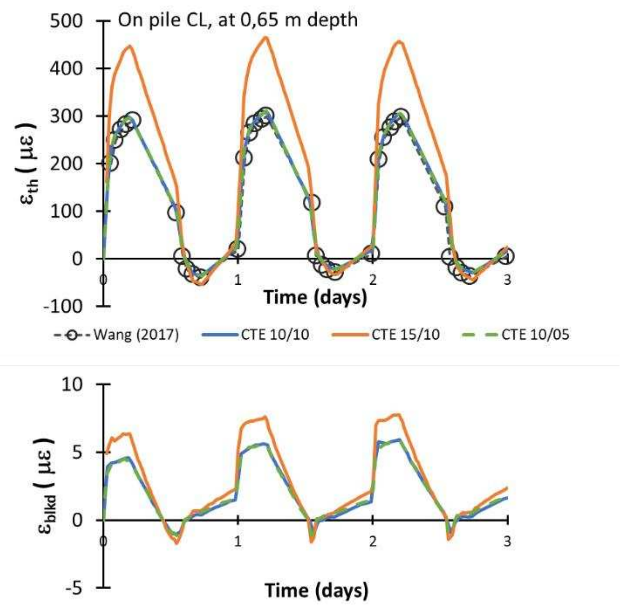

Figure 8. Thermal axial strain reported by Wang et al. (2017) and predicted by FEA using MC soil model.

The associated thermal stress response is shown in Figure 9 where clear discrepancies between the reported values and the FEA can be noted. This belies the good agreement between the reported and back-analysed results presented above. However, given that the thermal stress is evaluated using Eq. (2) in which errors accumulate through each of the experimental input parameters (ε_{th} & T), and the difference inside the square brackets (ε_{blkd}) is small (see Figure 8), large differences can be expected;

$$\sigma_{th} = E[\varepsilon_{th} - \alpha(T - T_0)] \tag{2}$$

To test this further, the 800 to 900 kPa axial stress reported by Wang (2017) implies an axial load of 6.8 to 7.7 kN which is higher than the total available shaft resistance implied by the load test discussed earlier (less than 2 kN). Based on Wang (2016) and other works, the maximum thermal stress will occur a depth of 0.5L to 0.7L. Thus, to generate the axial restraint required, friction equivalent to about 32 kPa and 23 kPa, respectively, would need to be mobilised on the shaft. This is highly unrealistic given the very low confining pressures acting on the pile shaft and based on Eq. (3), implies β = 2.9 – 5.7, values only likely to be found for large-displacement piles in sand;

$$\beta = {q_{s,u}}/{\bar{\sigma}'_v} \tag{3}$$

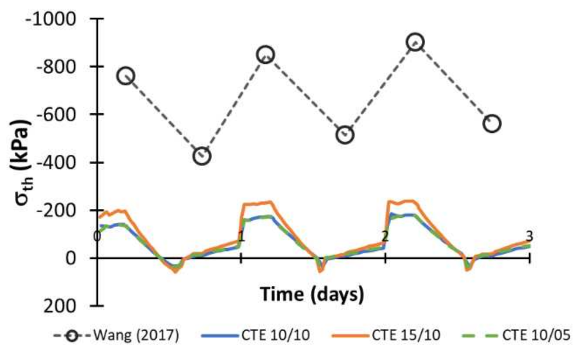

Figure 9. Thermal axial stress response reported by Wang et al. (2017) and predicted by FEA using MC soil model.

The other key parameter in TA pile response is the pile head movement and the reported values are compared with those predicted by the FEA in Figure 10. It is apparent that in terms of $y_{0,th}$, in the first cycle and subsequent heating stages, the agreement is good for case CTE 10/10. However, in the cooling stages, while the behaviour is qualitatively similar, the accumulated settlement diverges from and is less than that reported.

To assess this, a series of analyses were undertaken to investigate how the CTE affected the results. In Figure 10, results from analyses where the CTE of the pile was increased by 50% (CTE 15/10) and where the CTE of the soil was reduced by 50% (CTE 10/05) with respect to the initial values, are also shown. Again, the same pattern of accumulated settlement occurs: increasing the pile CTE improves the agreement with later cycles but at the cost of poor agreement in the first. Halving the soil CTE only affects the 2nd and 3rd cycles and marginally improves the predicted behaviour. Reducing the soil CTE further improves the match in the cooling cycles but the agreement during heating cycles deteriorates, underpredicting the reported values.

Table 2 and Figure 11 examine the reported thermally-induced pile settlement a little further. Table 2 summarises the incremental pile head movement and temperature change during each temperature change stage, i.e. Initial → H1 → C1 →… Also tabulated is the associated free thermal expansion, $y_{th,free}$ based on the average pile temperature and CTE reported by Wang et al. (2017).

What is clear in Table 2 is that within each cooling cycle, the pile head moves down by an amount approximately equal to $y_{th,free}$, while in the heating stages the pile head moves up and the proportion of $y_{th,free}$ mobilised increases with each heating stage. Figure 11 illustrates schematically what is thought to be happening; when heated the pile expands, reversing the friction in the upper part of the pile and thus, $y_{0,th} < y_{th,free}$. At the base of the pile, the pile expansion leads to downwards movement. When cooled, additional shaft resistance cannot be mobilised, and to maintain equilibrium, the pile base settles some more. After the first cycle, this repeats throughout the test, leading to the thermal ratcheting effect that was reported in Wang et al. (2016, 2017) and predicted by the FEA.

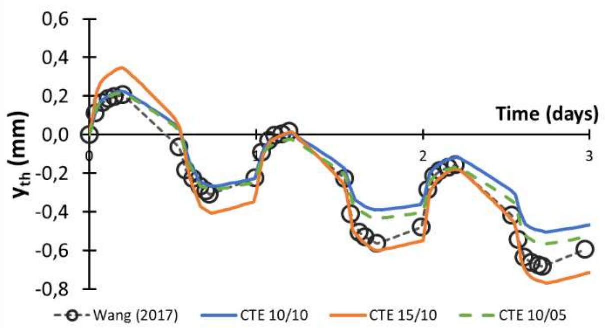

Figure 10. Thermal pile head displacement reported by Wang et al. (2017) and predicted by FEA using MC soil model.

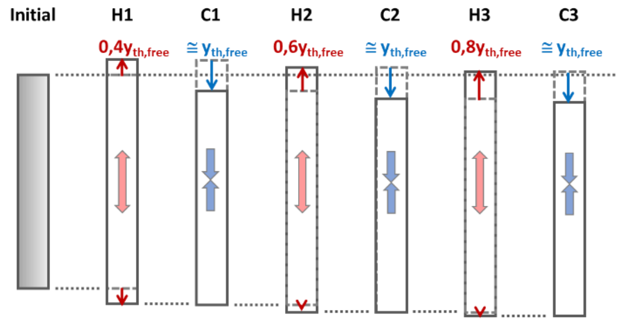

Figure 11. Schematic of pile thermal ratcheting mechanism.
.

Table 1. Material parameters used in analysis.

Parameter	Units	Pile	Sand
			MC Model
Density, ρ	kg/m^3	2500	1600
Young's modulus, E_{ref}	MPa	30000	20
Modulus increment, E_{inc}	MPa		14
Poisson's ratio, ν	-	0.2	0.3
Angle of shearing resistance, φ'	deg.	-	34
Angle of dilation, ψ	deg.	-	6
Cohesion, c'	kPa	-	0
Pile-soil interface friction, δ	deg.	-	29
Interface factor, $R_{inter} = \tan\delta/\tan\varphi'$	-	-	0.822
At-rest earth pressure coeff., K_0	-	-	1.0
Thermal conductivity, k	W/m.K	1.6	0.3
Specific heat, c_s	J/kg.K	880	830
Linear coeff. thermal expansion, α	x10^{-6} K^{-1}	varies	10
Initial temperature, T_0	°C	12	12

Table 2. Analysis of thermally-induced incremental pile head displacements.

Stage	Initial	H1	C1	H2	C2	H3	C3
$y_{0,th}$ (mm)	-	+0.21	-0.52	+0.33	-0.58	+0.41	-0.53
T (°C)	12.0	42.4	8.5	43.7	9.7	43.3	9.1
ΔT (°C)	-	+30.4	-33.9	+35.3	-34.0	+33.6	-34.2
L = 1600 mm, α = 10 x10^{-6} K^{-1}							
αΔT.L (mm)	-	+0.43	-0.48	+0.49	-0.48	+0.47	-0.48
$y_{0,th}$/αΔT.L	-	0.43	0.96	0.59	1.07	0.76	0.97

4 CONCLUSIONS

In this work, the behaviour of a small scale thermally-activated pile has been examined using the finite element method, employing two well known and commonly employed soil models. The following points have been demonstrated in this work:

- The mechanical load-displacement of the pile must be reproduced accurately in order to be able to reproduce the correct thermo-mechanical response.
- Good agreement between the test and analysis was found in terms of the thermal axial strains and pile head movements during heating.
- The results diverged in the cooling stages beyond the first cycle. The cause of this is not yet apparent, as e.g., a mechanism involving thermal compaction of the soil adjacent to the pile might improve this comparison but would likely no longer capture the movements during heating.
- The comparison between reported and predicted thermal stress was also poor. This may be due to the low levels of restraint on the pile shaft which means slight errors greatly exaggerate the blocked thermal strain and thus, the thermal stress reported. It is shown that the reported axial stress is likely to be unreliable.

ACKNOWLEDGEMENTS

The work presented was financed by the *Fundação para a Ciência e a Tecnologia*, Portugal, via grants PTDC/ECI-EGC/29083/2017 (DEEPCOOL) and UIDB/04625/2020. The authors would like to express their gratitude to the funding institution

REFERENCES

Bolton, M.D., (1987). Discussion: The strength and dilatancy of sands. *Géotechnique* 37, 219–226. https://doi.org/10.1680/geot.1987.37.2.219.

Bolton, M.D., (1986). The strength and dilatancy of sands. *Géotechnique* 36, 65–78. https://doi.org/10.1680/geot.1986.36.1.65.

Boulon, M., Foray, P., (1986). Physical and numerical simulations of lateral shaft friction along offshore piles in sand, in: *Proc. 3rd Int. Conf. on Numerical Methods in Offshore Piling*. Nante, France, pp. 127–147.

Bourne-Webb, P.J., Bodas Freitas, T.M., Freitas Assunção, R.M., (2019). A review of pile-soil interactions in isolated, thermally-activated piles. *Computers and Geotechnics* 108, 61–74. https://doi.org/10.1016/j.compgeo.2018.12.008.

Bourne-Webb, P.J., Bodas Freitas, T.M., (2020). Thermally-activated piles and pile groups under monotonic and cyclic thermal loading–A review. *Renewable Energy* 147, 2572–2581. https://doi.org/10.1016/j.renene.2018.11.025.

Bourne-Webb, P.J., Lupattelli, A., Bodas Freitas, T.M., Salciarini, D. (2022a). The influence of initial shaft resistance mobilisation in the response of seasonally, thermally-activated pile foundations in granular media. *Geomechanics for Energy and the Environment* 32, 100299. https://doi.org/10.1016/j.gete.2021.100299.

Bourne-Webb, P.J, Freitas, T.M.B., Zito, M., Lupattelli, A., Sterpi, D., Salciarini, D., (2022b). Outstanding issues in understanding the behaviour of thermally-activated pile foundations. *DFI-EFFC Intl. Conf. on Deep Foundations and Ground Improvement*, Berlin, Germany, p. 10.

Iwasaki, T., Tatsuoka, F. (1977). Effects of Grain Size and Grading on Dynamic Shear Moduli of Sands. Soils and Foundations 17, 19–35. https://doi.org/10.3208/sandf1972.17.3_19.

Jaky, D.J. (1948). Pressure in silos. Proc. 2nd Intl. Conf. Soil Mech. and Fdtn. Eng'g, Rotterdam, Vol. 1, 103-107. https://www.issmge.org/uploads/publications/1/43/1948_01_0021.pdf (accessed: 04/03/2024).

Mayne, P.W. (2000). Enhanced geotechnical site characterization by seismic piezocone penetration tests. *4th Intl. Geotech. Conf.*, Cairo, Egypt, pp. 95–120.

Nguyen, V.T., Tang, A.M., Pereira, J.-M. (2017). Long-term thermo-mechanical behavior of energy pile in dry sand. *Acta Geotech*. 12, 729–737. https://doi.org/10.1007/s11440-017-0539-z.

Rotta Loria, A.F., Donna, A.D., Laloui, L. (2015). Numerical Study on the Suitability of Centrifuge Testing for Capturing the Thermal-Induced Mechanical Behavior of Energy Piles. *J. Geotech. Geoenviron. Eng*. 141, 04015042. https://doi.org/10.1061/(ASCE)GT.1943-5606.0001318.

Wang, C., Liu, H., Kong, G., Ng, C.W.W., Wu, D. (2016). Model tests of energy piles with and without a vertical load. *Environmental Geotechnics* 3, 203–213. https://doi.org/10.1680/jenge.15.00020.

Wang, C., Liu, H., Kong, G., Wang Wai Ng, C. (2017). Different types of energy piles with heating–cooling cycles. *Proceedings of the Institution of Civil Engineers - Geotechnical Engineering* 170, 220–231. https://doi.org/10.1680/jgeen.16.00061.